European Radiology (2020) 30:3178–3187
https://doi.org/10.1007/s00330-020-06660-9

ULTRASOUND

Increased carotid artery wall stiffness and plaque prevalence in HIV infected patients measured with ultrasound elastography

Marie-Hélène Roy Cardinal[1] · Madeleine Durand[2,3] · Carl Chartrand-Lefebvre[4,5] · Claude Fortin[6] · Jean-Guy Baril[7] · Benoit Trottier[7] · Jean-Pierre Routy[8] · Gilles Soulez[4,5,9] · Cécile Tremblay[6,10] · Guy Cloutier[1,5,9]

Received: 3 September 2019 / Revised: 17 December 2019 / Accepted: 17 January 2020 / Published online: 12 February 2020

Abstract

Objectives Assess carotid artery strain and motion in people living with HIV as markers of premature aging using ultrasound noninvasive vascular elastography (NIVE).

Methods Seventy-four HIV-infected and 75 age-matched control subjects were recruited from a prospective, controlled cohort study from October 2015 to October 2017 (mean age 56 years ± 8 years; 128 men). NIVE applied to longitudinal ultrasound images of common and internal carotid arteries quantified the cumulated axial strain, cumulated shear strain, cumulated axial translation, and cumulated lateral translations. The presence of plaque was also assessed. An association between elastography biomarkers and HIV status was evaluated with Mann–Whitney tests and multivariable linear regression models.

Results A higher occurrence of carotid artery plaques was found in HIV-infected individuals ($p = 0.011$). Lower cumulated lateral translations were found in HIV-infected subjects on both common and internal carotid arteries ($p = 0.037$ and $p = 0.026$, respectively). These observations remained significant when considering multivariable models including common cardiovascular risk factors and clinical characteristics ($p < 0.05$). Lower cumulated axial strains were also observed in internal carotid arteries when considering both multivariable models ($p < 0.05$).

Conclusion Lower translation and strain of the carotid artery wall in HIV-infected individuals indicates increased vessel wall stiffness. These new imaging biomarkers could be used to characterize premature atherosclerosis development.

Key Points

- *Noninvasive vascular elastography (NIVE) based on ultrasound imaging quantifies translations and strains of carotid arteries.*
- *Lower translation and strain of the carotid artery wall found in HIV-infected individuals indicate premature arterial stiffening, compared with age-matched controls.*
- *Carotid artery plaques were more prevalent in HIV-infected individuals than in control subjects.*

Electronic supplementary material The online version of this article (https://doi.org/10.1007/s00330-020-06660-9) contains supplementary material, which is available to authorized users.

✉ Guy Cloutier
guy.cloutier@umontreal.ca

[1] Laboratory of Biorheology and Medical Ultrasonics, University of Montreal Hospital Research Center (CRCHUM), Montréal, QC H2X 0A9, Canada

[2] Department of Internal Medicine, University of Montreal Hospital Center (CHUM), Montréal, QC H2X 0C1, Canada

[3] Department of Medicine, University of Montreal, Montréal, QC, H3T 1J4, Canada

[4] Department of Radiology, University of Montreal Hospital Center (CHUM), Montréal, QC H2X 0C1, Canada

[5] Department of Radiology, Radio-Oncology and Nuclear Medicine, University of Montreal, Montréal, QC H3T 1J4, Canada

[6] Department of Medical Microbiology and Infectiology, University of Montreal Hospital Center (CHUM), Montréal, QC H2X 0C1, Canada

[7] Clinique Médicale Urbaine du Quartier Latin, Montréal, QC H2I 4E9, Canada

[8] Chronic Viral Illness Service, McGill University Health Centre, Montréal, QC H4A 3J1, Canada

[9] Institute of Biomedical Engineering, University of Montreal, Montréal, QC H3T 1J4, Canada

[10] Department of Microbiology, Infectiology and Immunology, University of Montreal, Montréal, QC H3T 1J4, Canada

Keywords HIV infections · Premature aging · Ultrasonography · Carotid arteries · Elasticity imaging techniques

Abbreviations

ART	Antiretroviral therapy
CAS	Cumulated axial strain
CAT	Cumulated axial translation
CCA	Common carotid artery
CHACS	Canadian HIV and Aging Cohort Study
CLT	Cumulated lateral translation
C|ShS|	Cumulated axial shear magnitude
HDL-C	High-density lipoprotein cholesterol
ICA	Internal carotid artery
IMT	Intima-media thickness
LDL-C	Low-density lipoprotein cholesterol
NIVE	Noninvasive vascular elastography

Introduction

Antiretroviral therapy (ART) has considerably changed the human immunodeficiency virus (HIV) epidemiology, transforming this infection into a chronic manageable disease. HIV-infected subjects live longer, with an estimated life expectancy of 20–50 years following infection [1–3]. However, they still have a shorter life expectancy and have higher rates of diseases than the general population that are nonrelated to HIV infection [4, 5]. Some of these diseases seem to be related to premature aging, including cardiovascular diseases, bone metabolism disorder, dyslipidemia, diabetes, and neurocognitive disorders. Premature aging has also been observed in HIV-infected children [6]. HIV infection is associated to altered immunity, drug toxicity, lifestyle (e.g., smoking), and sustained low-grade inflammatory activity [7]. In the case of cardiovascular diseases, the risk of developing coronary heart disease is increased by 1.5 to 2.0 compared to control subjects [8]. Higher prevalence of cardiomyopathy and diastolic dysfunction and increased left ventricular mass were also reported [9].

The carotid artery intima-media thickness (IMT) evaluated in B-mode ultrasound (US) is a recognized biomarker of early atherosclerosis [10] but has a moderate association with cardiovascular risk related to HIV serostatus [11]. Moreover, the association between IMT and stroke risk has been denied in the general population [12, 13]. Nevertheless, greater carotid artery IMT was found in HIV-infected individuals [14], and this metric was reported to increase after the initiation of antiretroviral therapy [15].

As an alternative to IMT, carotid vessel wall displacement and strain elastography caused by the pulsating blood vessel [16–18] and carotid artery stiffness parameters [19, 20] have been proposed as new biomarkers of early atherosclerosis. Strain elastography was also used to study mechanical properties of carotid artery plaques [21–26]. Whereas wall displacement and strain have not yet been reported in the HIV population, other US measures of artery mechanics have been documented. Lower distensibility and compliance of carotid and femoral arteries were found in HIV-infected patients [14]. Pulse waveform analysis also showed lower elasticity of large and small arteries in untreated HIV-infected subjects compared with HIV-negative participants [27]. In HIV-infected women, cellular markers of immune activation were associated with increased carotid artery stiffness (low distensibility and high Young's moduli), as measured with B-mode US [28, 29]. An association between increased arterial stiffness (higher pulse wave velocity) and duration of antiretroviral therapy was found [30].

Noninvasive vascular elastography (NIVE) provides time-varying images of vessel wall axial and lateral translations, axial strain, and shear strain overlaid on B-mode images of the vessel wall to characterize carotid artery biomechanics. In comparison, distensibility and compliance are based on lumen diameter changes, and pulse wave velocity is a global arterial tree stiffness assessment. NIVE measurements can also be made in plaques or in the internal carotid artery wall in addition to the common carotid artery wall. In a previous report, carotid artery premature stiffening was detected with NIVE using translation and strain features in a population of children with elevated body mass index (BMI) [18].

Since arterial stiffening is expected in the HIV population, the objective of this study was to detect premature aging of carotid arteries in HIV-infected individuals using carotid artery wall displacement and strain maps computed with NIVE. To detect premature biomechanical changes, our study considered participants with low or intermediate cardiovascular risk.

Methods

Study participants

Subjects were recruited from the Canadian HIV and Aging Cohort Study (CHACS), which has been described in detail elsewhere [31]. Briefly, inclusion criteria for the CHACS included either being ≥ 40 years of age or having lived with HIV infection for 15 years or more and having a life expectancy of at least 1 year. Representative population controls were selected by recruiting HIV-negative patients that attended the same hospital and community clinics as HIV-positive patients. Recruitment was made using frequency matching for age

and sex between HIV-positive and HIV-negative groups. In addition, other eligibility criteria to be included in the present preplanned carotid US substudy was a low or intermediate cardiovascular risk (10-year Framingham score of 5% to 20%) and absence of history or symptoms of coronary artery disease. Prospectively collected data on all clinically defined confounders of interest were obtained from the CHACS central database.

This study has received approval from the institutional review board on ethics at the Centre Hospitalier de l'Université de Montréal. Written informed consent was obtained from all participants.

Ultrasound imaging

US acquisitions were performed between October 2015 and October 2017. Arterial walls of left and right common and internal carotids were assessed in this study; 4 cine-loops were thus acquired for each patient. Longitudinal views of each vessel were acquired with an Aixplorer system (SuperSonic Imagine) using a 256-element linear array probe (SuperLinear™ SL15-4) at 7.5 MHz. Patients were asked to hold breath during acquisitions. The frame rate was set to 50 frames per s, and cine-loops of raw US radiofrequency data were recorded for approximately 5 s. Examinations were performed by a vascular technologist with more than 20 years of experience.

Image analysis

B-mode cine-loops were reconstructed from radiofrequency images using a Hilbert transform and logarithm compression. Pixel size of reconstructed B-mode images was 20.5 μm axially × 200 μm laterally (axial indicates direction of the US beam, and lateral means direction perpendicular to it). A semi-automated segmentation method was used to delineate a normal portion of the carotid far wall (without plaque or calcium) on all frames of B-mode cine-loops [32]. Plaques, defined as an IMT greater than 1 mm, were also delineated on near and/or far wall if present. To initialize segmentation, carotid wall contours were manually segmented on a single B-mode image that was selected by an experienced technician. All manual segmentations done by the technician were verified by a radiologist with more than 20 years of experience in vascular imaging. The carotid artery IMT was computed from automated segmentations as the mean distance between two segmented carotid wall contours (lumen-intima and media-adventitia interfaces). This metric was determined on all segmented frames and then averaged for each 5-s cine-loop; IMTs of left and right sides were then averaged. All segmentations were performed blinded to elastography results. Image assessors were blinded to the HIV status. Moreover, the presence of wall or plaque calcification with visible acoustic shadowing was noted, along with Doppler resistivity indices. Finally, the distensibility and compliance coefficients were computed in the common carotid artery [33]; for each subject, coefficients from left and right sides were averaged.

Elastograms induced by the natural cardiac pulsation were determined in each cine-loop between a pair of consecutive time-varying radiofrequency images to assess mechanical properties of carotid artery walls and existing plaques [34, 35]. Elastography cine-loops of axial and lateral translation motions, axial strains, and axial shear strains were computed. Translations are rigid displacements, axial strain corresponds to a compression or dilation of the vessel wall, and shear strain measures an angular change of shape (from rectangle to parallelogram) of the vessel wall. For each mechanical parameter, time-varying curves were computed by spatially averaging over the segmented carotid artery wall, each elastogram frame of the cine-loop [22, 36]. Descriptive elastography features, namely the cumulated axial strain (CAS), cumulated axial shear magnitude (C|ShS|), cumulated axial translation (CAT), and cumulated lateral translation (CLT), were computed from these time-varying curves. A time point on cumulated curves corresponds to the sum of previous instantaneous measures (cumulated sums were reset to zero at each cardiac cycle). The terminology "cumulated" used for each biomarker means the range of variation of the cumulated curve over a cycle and quantifies the total strain or translation occurring during that cycle. Examples of elastograms and of time-varying elastography curves are displayed in Fig. 1 for CAS and C|ShS| and in Fig. 2 for CAT and CLT. In a given participant with the presence of atherosclerosis, separate elastograms were obtained in regions with plaques, in addition to elastograms of the normal wall.

The ultrasound radiofrequency data processing and B-mode image segmentation methods were implemented in-house in a commercial imaging platform (Visual-NIVE, Object Research Systems).

Statistical analyses

Each statistical test was performed with R software (version 3.2.5; R Foundation for Statistical Computing, https://www.r-project.org). Descriptive statistics are reported as means ± standard deviations (SDs). Comparisons between clinical characteristics of HIV-infected and control subjects were done using Student's *t* tests (or Mann–Whitney test when data was not normally distributed according to Shapiro–Wilk test), and the chi-square test was used for categorical variables. For each of carotid artery walls (common and internal), elastography features from left and right sides were averaged and then compared between infected and control subjects with Mann–Whitney tests. All statistical analyses were performed separately for common and internal carotid arteries.

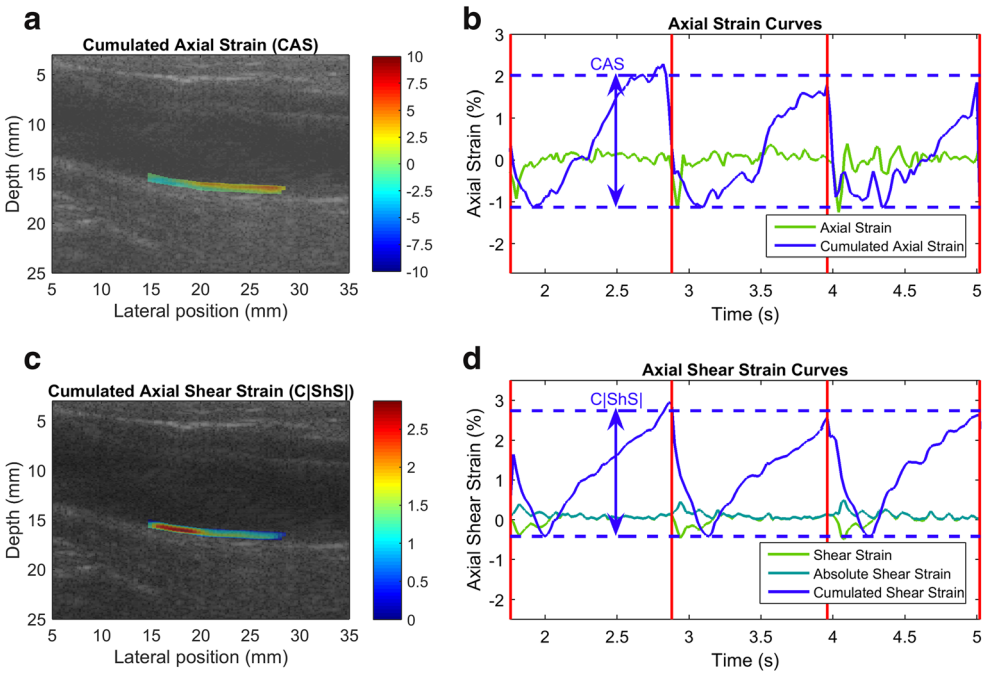

Fig. 1 Common carotid artery of a 45-year-old HIV-infected man. Two-dimensional longitudinal B-mode images reconstructed from radiofrequency data with cumulated axial strain (**a**) and cumulated axial shear strain (**c**) superimposed on segmented far wall of the carotid artery; strains were cumulated during systolic compression. Color maps depict strain in percentage (%). Panels **b** and **d** show time-varying elastogram curves of axial strain and axial shear strain, respectively. Cardiac cycles are delimited by red lines on panels **b** and **d**. For display purpose, panels **a** and **c** show elastograms cumulated during the diastolic phase of the first cardiac cycle

Simple linear regression models were first applied to compare elastogram measurements between groups. Two multivariable linear regression models adjusted for different confounders were then used to evaluate associations between elastography features of common and internal carotid arteries and HIV infection status. The first multivariable model included cardiovascular risk factors of sex, age, high waist circumference, high blood pressure, smoking status, and low-density lipoprotein cholesterol (LDL-C); the pulse pressure (systolic–diastolic blood pressure) was also considered in the first model since the same vessel would present higher translations and strains with a higher pulse pressure. The second multivariable model included all clinical characteristics that differed between groups (see Table 1). In all models, HIV status was the main exposure and elastography features were the outcome variables.

Carotid artery plaques were processed separately since they were not present in all subjects. The proportion of individuals with plaques was compared in both groups (simple and multivariable model 1 and 2 analyses). When plaques were

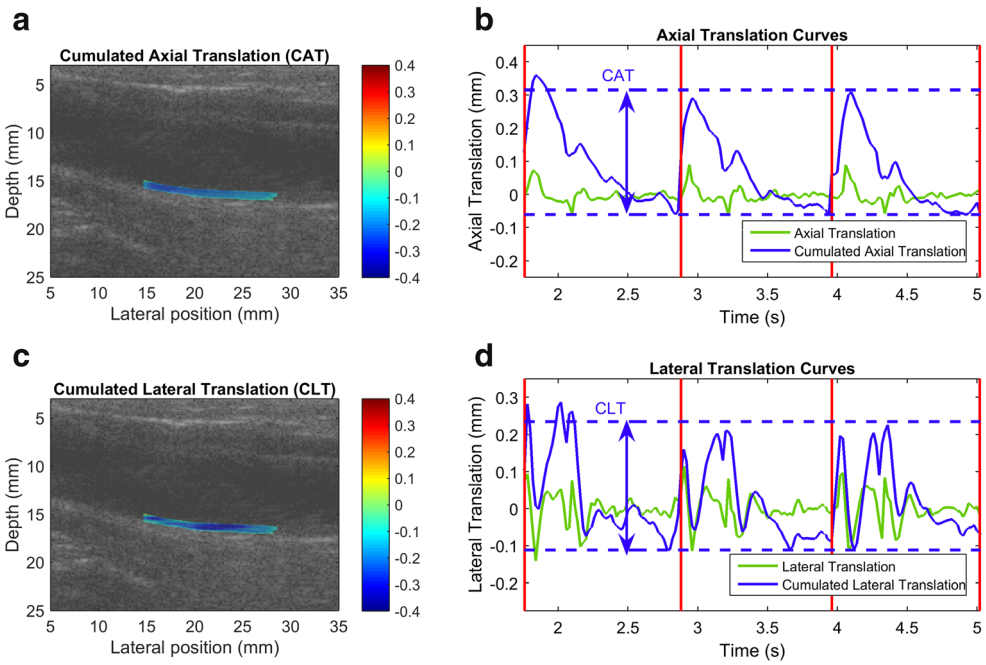

Fig. 2 Common carotid artery of a 45-year-old HIV-infected man. Two-dimensional longitudinal B-mode images reconstructed from radiofrequency data with cumulated axial translation (**a**) and cumulated lateral translation (**c**) superimposed on segmented far wall of the carotid artery; translations were cumulated during systolic compression. Color maps depict translation in millimeters (mm). Panels **b** and **d** show time-varying elastogram curves of axial and lateral translations, respectively. Cardiac cycles are delimited by red lines on panels **b** and **d**. For display purpose, panels **a** and **c** show elastograms cumulated during the diastolic phase of the first cardiac cycle

Table 1 Population characteristics of HIV-infected and control groups

	Total ($N = 149$)	HIV infected ($N = 74$)	Control ($N = 75$)	p value
Male (number)*	128 (86%)	70 (95%)	58 (77%)	*0.0052*¥
Age (years)†	56 ± 8	56 ± 7	56 ± 8	0.740
Framingham Risk Score‡	10.8 ± 5.3	11.0 ± 6.3	10.5 ± 4.4	0.884
High waist circumference*	42 (28%)	15 (20%)	27 (36%)	*0.045*¥
Diabetes*	5 (3%)	3 (4%)	2 (3%)	0.988
Hypertension*	38 (26%)	21 (28%)	17 (23%)	0.541
Statin usage*	33 (22%)	22 (30%)	11 (15%)	*0.044*¥
Smoking status*				
Current smoker	26	18	8	*0.029*¥
Former smoker (years since quitting)	61 (22 ± 14)	31 (22 ± 14)	30 (23 ± 14)	
No smoker	60	23	37	
NA	2	2	0	
Smoking history (pack-years)‡	10.5 ± 16.8	14.6 ± 20.3	6.6 ± 11.3	*0.0053*¥
Physical activity*				
30 min, daily	63 (42%)	29 (39%)	34 (45%)	*4.40e−4*¥
30 min, 3 times a week	30 (20%)	8 (11%)	22 (29%)	
30 min, weekly	10 (7%)	3 (4%)	7 (9%)	
No physical activity	42 (28%)	31 (42%)	11 (15%)	
NA	4 (3%)	3 (4%)	1 (1%)	
Family history of cardiovascular diseases*	116 (78%)	59 (80%)	57 (76%)	0.726
Blood biochemistry‡				
LDL-C	3.05 ± 0.95	2.88 ± 1.03	3.20 ± 0.86	*0.013*¥
HDL-C	1.34 ± 0.37	1.27 ± 0.35	1.41 ± 0.38	*0.016*¥
Creatinine‡	79 ± 14	82 ± 14	76 ± 14	*0.0028*¥
Blood pressure before US (mmHg)				
Systolic‡	121 ± 10	121 ± 11	121 ± 10	0.675
Diastolic‡	76 ± 9	77 ± 8	75 ± 9	0.399
Pulse pressure‡	45 ± 7	44 ± 8	46 ± 6	0.140
Presence of carotid artery plaque*	45 (30%)	30 (40%)	15 (20%)	*0.011*¥
Presence on one side only	32 (71%)	20 (67%)	12 (80%)	
Presence on left and right sides	13 (29%)	10 (33%)	3 (20%)	
Presence of calcium in the carotid artery wall*	25 (17%)	16 (21%)	9 (13%)	0.175
Doppler resistivity index†				
Common carotid artery	0.76 ± 0.04	0.75 ± 0.04	0.76 ± 0.04	0.450
Internal carotid artery	0.63 ± 0.05	0.63 ± 0.05	0.63 ± 0.05	0.655
Distensibility coefficient ($kPa^{-1} \times 10^{-3}$)	14.5 ± 4.4	14.6 ± 4.6	14.3 ± 4.1	0.84
Compliance coefficient (mm^2/kPa)	0.92 ± 0.30	0.94 ± 0.31	0.91 ± 0.30	0.74
HIV duration (years)		18 ± 8	NA	
Any exposure to ARV		67 (91%)		
ART duration (years)		14 ± 7	NA	
Nadir $CD4^+$ T-cell count ($cells/mm^3$)		249 ± 170	NA	
$CD4^+$ T-cell count ($cells/mm^3$)		591 ± 259	NA	
Ratio $CD4^+/CD8^+$		0.94 ± 0.50	NA	
Detectable viral load		1 (1%)	NA	
Exposure to NRTI		64 (86%)	NA	
Exposure to NNRTI		23 (31%)	NA	
Exposure to PI		29 (39%)	NA	
Exposure to INSTI		23 (31%)	NA	

High waist circumference is defined as over 102 cm in males or 88 cm in females; pack-years is the product of the number of packs of cigarettes smoked per day by the number of years the person has smoked; pulse pressure refers to systolic–diastolic blood pressure

NA not applicable/available, *LDL-C* low-density lipoprotein cholesterol, *HDL-C* high-density lipoprotein cholesterol, *ART* antiretroviral therapy, *NRTI* nucleoside reverse transcriptase inhibitor, *NNRTI* nonnucleoside reverse transcriptase inhibitor, *PI* protease inhibitor, *INSTI* integrase strand transfer inhibitor

*Pearson chi-square test

¥ Statistically significant at $p < 0.05$ (p values in italic emphasize significance)

† Independent sample Student's t test

‡ Mann–Whitney test

present on both left and right sides, their elastogram features were averaged.

Data in tables were not adjusted for multiple comparisons because elastogram features are not independent; a p value

< 0.05 indicated statistical significance. For multivariable analyses, the square root or logarithm transformation of elastogram features was used to achieve normalization of their data distribution; the transformation resulting in the highest Shapiro–Wilk test p value was applied. These transformations can reduce the impact of outliers and normalize skewed data [37]. Elastogram features are reported without transformation in the "Results" section.

Results

A total of 149 participants were recruited: 74 HIV-infected and 75 control subjects. Clinical characteristics and cardiovascular risk factors of these participants are presented in Table 1. There were statistically significant higher percentages of men and statin usage, a higher number of current smokers and smoking history, less physical activity, and higher creatinine levels in the HIV-infected group. They also had lower prevalence of high waist circumference and lower levels of LDL-C and HDL-C. No difference was found for other clinical characteristics. A higher prevalence of subjects with carotid artery plaques was observed in the HIV-infected group. Although different relative frequencies of the presence of calcium were observed (21% vs. 13%), they did not reach statistical significance ($p = 0.175$) neither did the Doppler resistivity indices ($p = 0.450$ and $p = 0.655$).

Table 2 reports elastography features that were computed. On simple analyses, statistically significant lower CLTs were found in HIV-infected subjects for both common and internal carotid arteries ($p = 0.037$ and $p = 0.026$, respectively). Other elastography features were not statistically different. On the other hand, there were statistically significant associations between internal carotid CAS, CAT, and CLT elastography features and HIV infection in multivariable model 1 ($p = 0.040$, $p = 0.044$, and $p = 0.015$, respectively). Internal carotid CAS and CLT were also significantly lower in the HIV-positive group according to multivariable model 2 ($p = 0.038$ and $p = 0.029$). Only CLT of the common carotid turned out to be statistically significantly lower in the HIV-infected group with both models ($p = 0.009$ and $p = 0.017$ for multivariable models 1 and 2, respectively). Neither IMT nor C|ShS| was significantly different between the two groups. The effect of confounding factors for multivariable models 1 and 2 can be found in the supplementary materials (Tables S1 and S2, respectively).

As shown in Table 1, 32 patients had one plaque and 13 had two plaques for a total of 58 plaques identified during US examinations. Multivariable logistic regressions were performed to test the prevalence of plaques between the two groups. The same covariates as models 1 and 2 (Table 2) were used. Plaque prevalence was still higher in the HIV-positive group ($p = 0.011$ in the simple analysis; $p = 0.032$ and $p = 0.005$ in multivariable models 1 and 2, respectively). Elastography results computed on plaques are reported in Table 3. There was no difference between elastography parameters of HIV-infected and noninfected subjects.

Discussion

HIV-infected individuals under ART live longer but develop premature aging and cardiovascular diseases. Prevention strategies for stroke risk stratification remain to be defined in this population. We have studied individuals living with HIV and having low or intermediate cardiovascular risk (Framingham score below 20%) and no history or symptoms of cardiovascular diseases.

The occurrence of carotid artery plaques was higher in HIV-infected individuals in simple and multivariable models; this was also observed in the study of Janjua et al [38]. A recent study has established that the presence of carotid artery plaques was associated with mortality in adults living with HIV who were free of clinical cardiovascular diseases [39], emphasizing the importance of early atherosclerosis detection and of cardiovascular disease management in aging HIV-positive individuals. Although increased IMT is a known marker for myocardial infarction and stroke in older adults without a history of cardiovascular diseases [40], new studies have shown that carotid plaque is more accurate than IMT for the prediction of future myocardial infarction [41]. In our study, IMT was not different between HIV-infected and noninfected groups. On the other hand, proposed mechanical imaging biomarkers based on NIVE allowed detection of stiffened carotid arteries in HIV individuals with low to moderate cardiovascular risk.

Lower lateral translations of common and internal carotid artery walls were observed in HIV compared with control subjects. It remained statistically significantly lower after including common cardiovascular risk factors (model 1) and after accounting for clinical variables that differed between groups (model 2). Similar associations were also found when using the minimum of elastography features between left and right carotid arteries corresponding to the side with stiffer arterial wall instead of averaging both features from left and right sides (see Table S3 in the supplementary materials). It has been shown previously that small lateral displacements of the common carotid artery assessed with US could be associated with established cardiovascular risk factors [16] and with greater occurrence of major adverse cardiovascular events [17]. A lower translation is an indicator of a stiffer carotid artery wall, which agrees with previous studies that measured artery stiffness globally using unidimensional methods providing distensibility, compliance, or pulse waveform velocity in HIV-infected populations [14, 27–30].

Table 2 IMT and elastography parameters of common carotid artery (CCA) and internal carotid artery (ICA) walls for HIV-infected (label +, $N = 74$) and uninfected (label −, $N = 75$) subjects

	Carotid segment	HIV status	Mean ± SD	p value (Mann–Whitney)	p value (multivariable model 1)	p value (multivariable model 2)
IMT	CCA	+	0.55 ± 0.07	0.113	0.167	0.164
		−	0.54 ± 0.06			
	ICA	+	0.53 ± 0.07	0.856	0.897	0.827
		−	0.53 ± 0.05			
CAS	CCA	+	2.94 ± 1.33	0.798	0.483	0.428
		−	2.84 ± 1.12			
	ICA	+	2.45 ± 1.28	0.067	*0.040*¥	*0.038*¥
		−	2.64 ± 0.95			
C|ShS|	CCA	+	2.53 ± 1.22	0.664	0.349	0.388
		−	2.56 ± 1.00			
	ICA	+	2.33 ± 0.83	0.251	0.132	0.197
		−	2.44 ± 0.72			
CAT	CCA	+	0.24 ± 0.08	0.467	0.081	0.089
		−	0.27 ± 0.11			
	ICA	+	0.17 ± 0.08	0.327	*0.044*¥	0.107
		−	0.19 ± 0.07			
CLT	CCA	+	0.40 ± 0.19	*0.037*¥	*0.009*¥	*0.017*¥
		−	0.45 ± 0.17			
	ICA	+	0.28 ± 0.16	*0.026*¥	*0.015*¥	*0.029*¥
		−	0.32 ± 0.13			

Model 1 was adjusted for sex, age, high waist circumference, high blood pressure, smoking status, LDL-C, and pulse pressure. Model 2 was adjusted for sex, high waist circumference, statin usage, smoking status, physical activity, LDL-C, HDL-C, and creatinine

IMT intima-media thickness (mm), *CAS* cumulated axial strain (%), *C|ShS|* cumulated axial shear strain magnitude (%), *CAT* cumulated axial translation (mm), *CLT* cumulated lateral translation (mm)

¥ Statistically significant at $p < 0.05$ (p values in italic emphasize significance)

The axial strain was also significantly lower in the internal carotid artery of HIV-infected individuals after taking into account confounding factors in both multivariable models. Lower carotid artery axial strain-to-displacement ratio was also observed in pediatric patients with obesity [18], using the same NIVE method as the current study. A lower axial strain also indicates a stiffer artery as less deformation is encountered with the pulse pressure.

Table 2 also shows that most elastography features of the common carotid artery did not differ between the HIV-infected and control subjects. Also, distensibility and compliance coefficients (Table 1) that are based on common carotid

Table 3 Elastography parameters of plaques for HIV-infected (label +, $N = 30$) and uninfected (label −, $N = 15$) subjects

	HIV status	Mean ± SD	p value (Mann–Whitney)	p value (multivariable model 1)	p value (multivariable model 2)
Plaque thickness (mm)	+	1.15 ± 0.32	0.073	0.129	0.100
	−	1.36 ± 0.40			
CAS	+	1.76 ± 1.01	0.253	0.262	0.281
	−	2.07 ± 0.92			
C|ShS|	+	2.74 ± 1.05	0.448	0.637	0.730
	−	2.94 ± 0.85			
CAT	+	0.18 ± 0.09	0.638	0.576	0.830
	−	0.18 ± 0.08			
CLT	+	0.39 ± 0.24	0.709	0.854	0.938
	−	0.39 ± 0.17			

Model 1 was adjusted for sex, age, high waist circumference, high blood pressure, smoking status, LDL-C, and pulse pressure. Model 2 was adjusted for sex, high waist circumference, statin usage, smoking status, physical activity, LDL-C, HDL-C, and creatinine

CAS cumulated axial strain (%), *C|ShS|* cumulated axial shear strain magnitude (%), *CAT* cumulated axial translation (mm), *CLT* cumulated lateral translation (mm)

artery diameter measurements were not different between groups. The following aims to provide reasons for the lack of discrimination between groups for common carotid artery measures. Indeed, it is known that carotid artery stenosis and occlusion predominantly occur at the bifurcation and internal carotid site [42]. Flow modifications at these sites due to changes in vessel geometry play a role in plaque development [43]. Further investigation would be necessary to show if internal carotid artery wall stiffness is an earlier marker of atherosclerosis than common carotid artery stiffness.

When comparing elastography measurements between carotid plaques of infected and uninfected subjects, there was no statistically significant difference (Table 3). However, only 45 subjects out of 149 had carotid artery plaques. Moreover, the higher statin usage in the HIV-infected group (Table 1) could have contributed in homogenizing the plaque tissue content and thus affecting plaque elastography measurements. Indeed, statin usage is known to change the carotid artery plaque composition by increasing the collagen content and reducing the lipid content, inflammation, metalloproteinases, and the cell death [44].

Limitations

Limitations of our study include its cross-sectional nature and one-time measurement of elastography parameters, although reverse causality is not an issue, as thickening and stiffening of the vascular wall cannot predispose to HIV infection. However, repeated measures over several years could help to quantify the relationship of HIV and its treatment to arterial wall rigidity.

A large discrepancy was present in the smoking history (pack-years) of both groups, and the number of current smokers was higher in the HIV-infected group. However, the majority of participants in both groups were either never-smokers or former-smokers with similar smoking cessation time. The confounding factor smoking status was taken into account as well as other important ones (age, sex, cholesterol levels, renal function) in the statistical models. Smoking history was not included in the models to prevent collinearity with the smoking status. However, other confounders, such as socioeconomic level, co-infections (cytomegalovirus, hepatitis), and the complex nature of the HIV antiretroviral therapy regimens, could not be completely captured in our data.

Sample size is another limitation. Because of the low sample size, an analysis limited to the HIV group did not yield statistically significant association between elastography measurements and HIV or ART duration, Nadir $CD4^+$ and $CD4^+$ T-cell counts, and ratio $CD4^+/CD8^+$ after multiple comparison adjustment. Instead of reporting multiple strain components, future studies could also focus on angle-independent principal strain measures to reduce the number of strain parameters [45]. A larger dataset might still be necessary to find such associations. Thus, HIV-related factors predicting increased arterial wall stiffness were not identified.

Finally, derived markers from elastography measurements are subclinical, and it is yet unclear if they will translate into an increased risk of overt cardiovascular disease. In this respect, the nesting of our study within the Canadian HIV and Aging Cohort Study [31] is a strength, as these patients benefit from a longitudinal follow-up with prospective assessment of cardiovascular events.

In conclusion, we have shown that carotid artery plaques were more frequent in HIV-infected individuals with low-to-intermediate cardiovascular risk. Their carotid artery walls were also stiffer as axial strains and displacements were smaller. Because age-matched populations were studied, carotid artery atherosclerosis thus seems to appear earlier in patients living with HIV. US elastography is noninvasive, is a local and time-varying imaging measurement of elasticity, and is not associated to radiation exposure. It will hopefully prove to be a valuable tool to detect premature atherosclerosis in patients living with HIV and ultimately help tailoring their therapeutic choices.

Funding information This study was initiated through the support of the Canadian Institute of Health Research (CIHR, Canadian HIV and Aging Cohort Study, group grant no. 284512); it is now supported by CIHR group grant no. 398643 and project grant no. 399544.

Compliance with ethical standards

Guarantor The scientific guarantor of this publication is Dr. Guy Cloutier.

Conflict of interest The authors declare that they have no conflict of interest.

Statistics and biometry Co-authors (MHRC, GS, and GC) have significant statistical expertise.

Informed consent Written informed consent was obtained from all subjects (patients) in this study.

Ethical approval Institutional review board approval was obtained.

Methodology
- prospective
- cross-sectional study
- performed at one institution

References

1. May MT, Gompels M, Delpech V et al (2014) Impact on life expectancy of HIV-1 positive individuals of CD4+ cell count and viral load response to antiretroviral therapy. AIDS 28:1193–1202
2. van Sighem AI, Gras LA, Reiss P, Brinkman K, de Wolf F (2010) Life expectancy of recently diagnosed asymptomatic HIV-infected

patients approaches that of uninfected individuals. AIDS 24:1527–1535
3. Antiretroviral Therapy Cohort Collaboration (2008) Life expectancy of individuals on combination antiretroviral therapy in highincome countries: a collaborative analysis of 14 cohort studies. Lancet 372:293–299
4. Deeks SG (2009) Immune dysfunction, inflammation, and accelerated aging in patients on antiretroviral therapy. Top HIV Med 17: 118–123
5. Guaraldi G, Orlando G, Zona S et al (2011) Premature age-related comorbidities among HIV-infected persons compared with the general population. Clin Infect Dis 53:1120–1126
6. Gianesin K, Noguera-Julian A, Zanchetta M et al (2016) Premature aging and immune senescence in HIV-infected children. AIDS 30: 1363–1373
7. Deeks SG, Phillips AN (2009) HIV infection, antiretroviral treatment, ageing, and non-AIDS related morbidity. BMJ 338:a3172
8. Vachiat A, McCutcheon K, Tsabedze N, Zachariah D, Manga P (2017) HIV and ischemic heart disease. J Am Coll Cardiol 69:73–82
9. Manga P, McCutcheon K, Tsabedze N, Vachiat A, Zachariah D (2017) HIV and nonischemic heart disease. J Am Coll Cardiol 69: 83–91
10. Bots ML, Hoes AW, Koudstaal PJ, Hofman A, Grobbee DE (1997) Common carotid intima-media thickness and risk of stroke and myocardial infarction: the Rotterdam Study. Circulation 96:1432–1437
11. Stein JH, Currier JS, Hsue PY (2014) Arterial disease in patients with human immunodeficiency virus infection: what has imaging taught us? JACC Cardiovasc Imaging 7:515–525
12. Lorenz MW, Polak JF, Kavousi M et al (2012) Carotid intima-media thickness progression to predict cardiovascular events in the general population (the PROG-IMT collaborative project): a meta-analysis of individual participant data. Lancet 379:2053–2062
13. Den Ruijter HM, Peters SA, Anderson TJ et al (2012) Common carotid intima-media thickness measurements in cardiovascular risk prediction: a meta-analysis. JAMA 308:796–803
14. van Vonderen MG, Smulders YM, Stehouwer CD et al (2009) Carotid intima-media thickness and arterial stiffness in HIV-infected patients: the role of HIV, antiretroviral therapy, and lipodystrophy. J Acquir Immune Defic Syndr 50:153–161
15. van Vonderen MG, Hassink EA, van Agtmael MA et al (2009) Increase in carotid artery intima-media thickness and arterial stiffness but improvement in several markers of endothelial function after initiation of antiretroviral therapy. J Infect Dis 199:1186–1194
16. Zahnd G, Vray D, Serusclat A et al (2012) Longitudinal displacement of the carotid wall and cardiovascular risk factors: associations with aging, adiposity, blood pressure and periodontal disease independent of cross-sectional distensibility and intima-media thickness. Ultrasound Med Biol 38:1705–1715
17. Svedlund S, Eklund C, Robertsson P, Lomsky M, Gan LM (2011) Carotid artery longitudinal displacement predicts 1-year cardiovascular outcome in patients with suspected coronary artery disease. Arterioscler Thromb Vasc Biol 31:1668–1674
18. El Jalbout R, Cloutier G, Roy Cardinal M-H et al (2019) The value of non-invasive vascular elastography (NIVE) in detecting early vascular changes in overweight and obese children. Eur Radiol 29:3854–3861
19. Cote AT, Phillips AA, Harris KC, Sandor GG, Panagiotopoulos C, Devlin AM (2015) Obesity and arterial stiffness in children: systematic review and meta-analysis. Arterioscler Thromb Vasc Biol 35:1038–1044
20. Zhu ZQ, Chen LS, Wang H et al (2019) Carotid stiffness and atherosclerotic risk: non-invasive quantification with ultrafast ultrasound pulse wave velocity. Eur Radiol 29:1507–1517
21. Shi H, Mitchell CC, McCormick M, Kliewer MA, Dempsey RJ, Varghese T (2008) Preliminary in vivo atherosclerotic carotid plaque characterization using the accumulated axial strain and relative lateral shift strain indices. Phys Med Biol 53:6377–6394
22. Naim C, Cloutier G, Mercure E et al (2013) Characterisation of carotid plaques with ultrasound elastography: feasibility and correlation with high-resolution magnetic resonance imaging. Eur Radiol 23:2030–2041
23. Hansen HH, de Borst GJ, Bots ML, Moll FL, Pasterkamp G, de Korte CL (2016) Validation of noninvasive in vivo compound ultrasound strain imaging using histologic plaque vulnerability features. Stroke 47:2770–2775
24. Roy Cardinal MH, Heusinkveld MHG, Qin Z et al (2017) Carotid artery plaque vulnerability assessment using noninvasive ultrasound elastography: validation with MRI. AJR Am J Roentgenol 209:142–151
25. Dempsey RJ, Varghese T, Jackson DC et al (2018) Carotid atherosclerotic plaque instability and cognition determined by ultrasound-measured plaque strain in asymptomatic patients with significant stenosis. J Neurosurg 128:111-119
26. Cloutier G, Roy Cardinal M-H, Ju Y, Giroux M-F, Lanthier S, Soulez G (2018) Carotid plaque vulnerability assessment using ultrasound elastography and echogenicity analysis. AJR Am J Roentgenol 211:847–855
27. Baker JV, Duprez D, Rapkin J et al (2009) Untreated HIV infection and large and small artery elasticity. J Acquir Immune Defic Syndr 52:25–31
28. Kaplan RC, Sinclair E, Landay AL et al (2011) T cell activation predicts carotid artery stiffness among HIV-infected women. Atherosclerosis 217:207–213
29. Karim R, Mack WJ, Kono N et al (2014) T-cell activation, both pre- and post-HAART levels, correlates with carotid artery stiffness over 6.5 years among HIV-infected women in the WIHS. J Acquir Immune Defic Syndr 67:349–356
30. Lekakis J, Ikonomidis I, Palios J et al (2009) Association of highly active antiretroviral therapy with increased arterial stiffness in patients infected with human immunodeficiency virus. Am J Hypertens 22:828–834
31. Durand M, Chartrand-Lefebvre C, Baril JG et al (2017) The Canadian HIV and aging cohort study—determinants of increased risk of cardio-vascular diseases in HIV-infected individuals: rationale and study protocol. BMC Infect Dis 17:611
32. Destrempes F, Meunier J, Giroux M-F, Soulez G, Cloutier G (2011) Segmentation of plaques in sequences of ultrasonic B-mode images of carotid arteries based on motion estimation and a Bayesian model. IEEE Trans Biomed Eng 58:2202–2211
33. Gamble G, Zorn J, Sanders G, MacMahon S, Sharpe N (1994) Estimation of arterial stiffness, compliance, and distensibility from M-mode ultrasound measurements of the common carotid artery. Stroke 25:11–16
34. Schmitt C, Soulez G, Maurice R, Giroux M, Cloutier G (2007) Noninvasive vascular elastography: toward a complementary characterization tool of atherosclerosis in carotid arteries. Ultrasound Med Biol 33:1841–1858
35. Maurice RL, Soulez G, Giroux MF, Cloutier G (2008) Noninvasive vascular elastography for carotid artery characterization on subjects without previous history of atherosclerosis. Med Phys 35:3436–3443
36. Mercure E, Destrempes F, Roy Cardinal MH et al (2014) A local angle compensation method based on kinematics constraints for non-invasive vascular axial strain computations on human carotid arteries. Comput Med Imaging Graph 38:123–136
37. Sheskin DJ (2011) Handbook of parametric and nonparametric statistical procedures, fifth edn. Chapman and Hall/CRC

38. Janjua SA, Staziaki PV, Szilveszter B et al (2017) Presence, characteristics, and prognostic associations of carotid plaque among people living with HIV. Circ Cardiovasc Imaging 10:e005777
39. Hanna DB, Moon JY, Haberlen SA et al (2018) Carotid artery atherosclerosis is associated with mortality in HIV-positive women and men. AIDS 32:2393–2403
40. O'leary DH, Polak JF, Kronmal RA, Manolio TA, Burke GL, Wolfson SK Jr (1999) Carotid-artery intima and media thickness as a risk factor for myocardial infarction and stroke in older adults. N Engl J Med 340:14–22
41. Inaba Y, Chen JA, Bergmann SR (2012) Carotid plaque, compared with carotid intima-media thickness, more accurately predicts coronary artery disease events: a meta-analysis. Atherosclerosis 220: 128–133
42. Hass WK, Fields WS, North RR, Kircheff II, Chase NE, Bauer RB (1968) Joint study of extracranial arterial occlusion. II. Arteriography, techniques, sites, and complications. JAMA 203: 961–968
43. Zarins CK, Giddens DP, Bharadvaj BK, Sottiurai VS, Mabon RF, Glagov S (1983) Carotid bifurcation atherosclerosis. Quantitative correlation of plaque localization with flow velocity profiles and wall shear stress. Circ Res 53:502–514
44. Crisby M, Nordin-Fredriksson G, Shah PK, Yano J, Zhu J, Nilsson J (2001) Pravastatin treatment increases collagen content and decreases lipid content, inflammation, metalloproteinases, and cell death in human carotid plaques: implications for plaque stabilization. Circulation 103:926–933
45. Nayak R, Schifitto G, Doyley MM (2018) Visualizing angle-independent principal strains in the longitudinal view of the carotid artery: phantom and in vivo evaluation. Ultrasound Med Biol 44: 1379–1391